MINERALOGICAL MAGAZINE, SEPTEMBER 1981, VOL. 44, PP. 287-91

Edge dislocations in fibrous grunerite

E. J. W. WHITTAKER AND B. A. CRESSEY

Department of Geology and Mineralogy, University of Oxford, Oxford, OX1 3PR

AND

J. L. HUTCHISON

Department of Metallurgy and Science of Materials, University of Oxford, OX1 3PH

ABSTRACT. Sections perpendicular to [001] of ion-thinned specimens of fibrous grunerite (amosite) have been examined by high-resolution transmission electron microscopy. In this orientation, two kinds of dislocation have been observed with about equal frequency. One lies on [001] and has a Burgers vector **a**. The other is on [001] and has a Burgers vector $\frac{1}{2}\mathbf{a}+\frac{1}{2}\mathbf{b}$. Interpretation of features associated with these dislocations has been assisted by the use of two-dimensional models of *I*-beam cross-sections which can be interlocked to simulate the possible modes of stacking.

IN a recent paper (Whittaker *et al.*, 1981) we have presented high-resolution electron micrographs of some terminations of lamellae of multiple chain *I*-beams, occurring in fibrous grunerite, that do not obey the 'termination rules' of Veblen and Buseck (1980). These 'incoherent terminations' were shown to involve distortions of the structure analogous to those in dislocations, as was also noted in one instance in anthophyllite by Veblen and Buseck (1980). In this paper we present observations of ordinary dislocations of standard type in the same specimens of fibrous grunerite.

Such ordinary dislocations do not seem to have been observed previously in amphibole. Hutchison *et al.* (1975) examined a number of fibrous amphiboles with the fibres lying flat on the microscope grid, but found no dislocations; nor have any dislocations been observed subsequently by other workers who have used this orientation (Veblen *et al.*, 1977; Jefferson *et al.*, 1978; Mallinson *et al.*, 1980). The non-observance of dislocations in these studies is readily interpreted in terms of the amphibole structure. The dislocations that could be revealed in orientations with the electron beam perpendicular to [001] would be as follows.

(i) Edge dislocations on [010] with Burgers vector **a** and on [100] with Burgers vector **b**. Either of these would involve termination of silicate chains along a [010] or [100] line, with a corresponding high density of broken bonds of high strength.

(ii) Edge dislocations on [010] with Burgers vector **c** and dislocations of predominantly edge-type on [100] with Burgers vector **c**. These would involve similarly high densities of broken bonds extending over several layers of silicate chains where these crossed the core of the dislocation.

The dislocations reported here were observed in electron micrographs looking along [001], and lie on this axis. Such dislocations involve much lower densities of broken bonds, which are also of lower strength. They are therefore much more likely to occur than dislocations on [100] or [010], although they have not hitherto been reported in other studies of amphibole in this orientation.

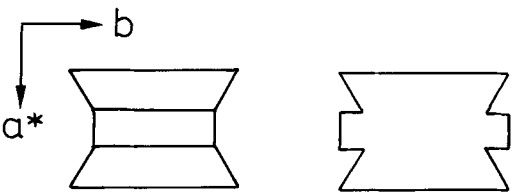

FIG. 1 (*left*). Conventional drawing of an amphibole *I*-beam. (*right*) The shape of the cardboard cut-out used for modelling stackings of *I*-beams.

In interpreting the electron micrographs we have again made use of interlocking cardboard cut-outs (Whittaker *et al.*, 1981) of '*I*-beam' cross-sections, using the now-standard nomenclature of Papike and Ross (1970). It is to be noted, however, that these cut-outs differ in shape from the standard representation of an amphibole *I*-beam, and from which the name is derived (fig. 1). This difference merits a brief consideration, because it is symptomatic of the existence of two ways of looking at the amphibole structure which has not generally been made explicit. If one dissects the amphibole structure (having empty *A*-sites) into isolatable units,

all of the same kind, then the unit is as shown in fig. 2 in terms of an atom-packing model These units are linked laterally by bonds between the cations *M*2 and *M*4 of one unit to peripheral oxygen atoms of adjacent units. Each *M*2 cation forms two such inter-unit bonds, and each *M*4 forms four or six. Since the *M*2 cation forms four bonds to oxygen atoms within the unit there is no doubt that it is correctly described as 'belonging' to this unit, but there is considerable doubt in the case of the *M*4 cation since it only forms two bonds to oxygen atoms within the unit. Furthermore, in a projection of the whole structure (fig. 3) it can be seen that the *M*4 ion lies rather more between the backs of the adjacent silicate chains than between the apical oxygen atoms of 'its own *I*-beam'. Indeed, in many descriptions of the structure the *I*-beams are said to be bonded back-to-back by *M*4 ions (as well as, where relevant, by ions in the *A*-sites). However, in descriptions of biopyribole structures in terms of CS planes (Chisholm, 1973) or of polysomatic series (Thompson, 1978) it is essential to regard the *M*4 cations as belonging to the same unit as the adjacent *M*2 cations. We have adopted this convention in designing the cardboard cut-outs for the practical reason that it makes the units interlock better and so

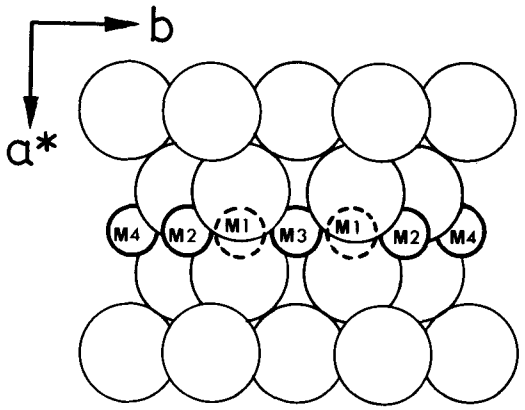

FIG. 2. Arrangement of atoms in a packing model of an amphibole.

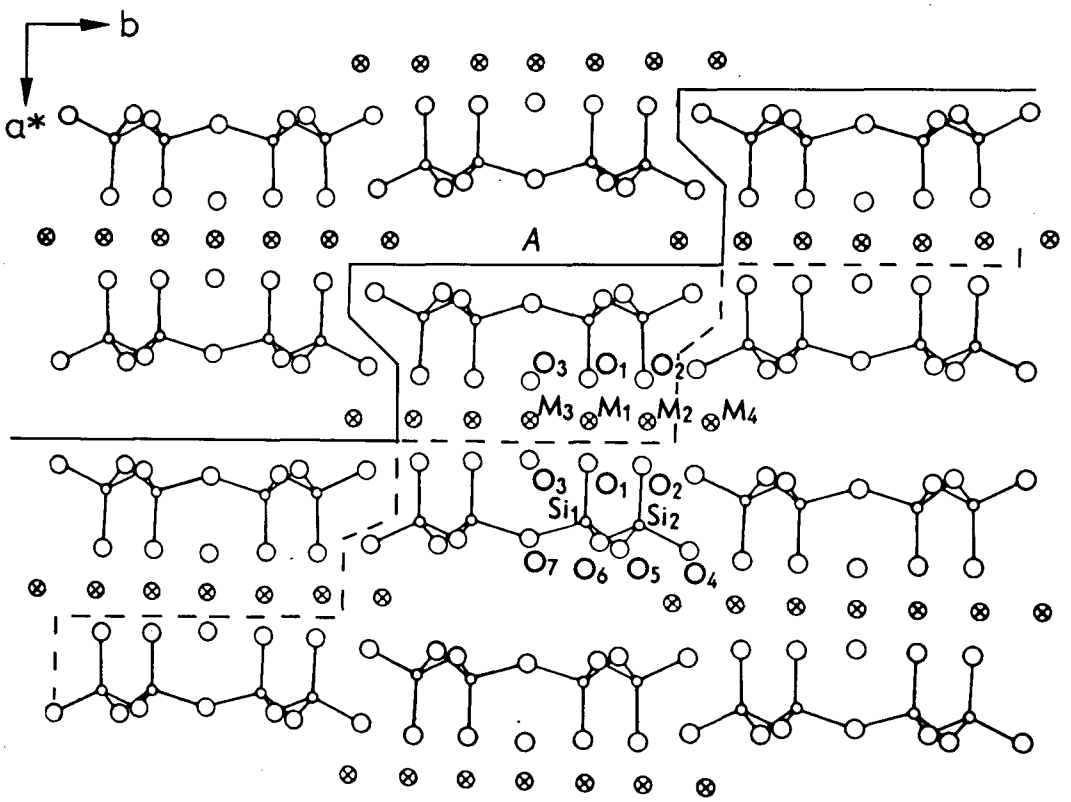

FIG. 3. Projection of the amphibole structure down the *c*-axis. The broken line shows the cleavage path according to Warren (1929), and the full line that according to Taylor (1959).

makes them easier to arrange, and also because drawings of stackings of *I*-beams of the form shown in fig. 1*b*, as, for example, in Veblen and Buseck (1980), necessarily omit any indication of the *M*4 cations and could therefore have misleading implications.

In passing, it may be noted that the formulation of the amphibole structure (and other biopyribole chain structures) in terms of a stacking of *I*-beams calls into question the interpretation of the cleavage by Warren (1929), and repeated many times since (see, for example, Buseck and Iijima, 1974). This is shown in fig. 3. It divides the structure between silicate chains, but it involves the breakage of *I*-beam units. As has been pointed out by Taylor (1959), the alternative path shown in fig. 3 involves much less bond-breaking. In fact, the former involves breaking 34 *M*-O bonds per unit cell intersected, whereas the latter only involves breaking 8 *M*-O bonds per unit cell, and 4 of these are 'residual bonds' from *M*4 to bridging oxygen atoms (05 and 06 in conventional nomenclature) that are already bonded to two silicon atoms each.

The specimens of fibrous grunerite from Penge, Transvaal, were identical with those described by Whittaker *et al.* (1981). They consisted of ion-thinned cross-sections perpendicular to the *c*-axis and the conditions of observation were as described in that paper.

The micrographs obtained are generally similar in nature to those of other amphiboles in this orientation obtained by Buseck and Iijima (1974), Alario Franco *et al.* (1977), Veblen *et al.* (1977), and Veblen and Buseck (1979, 1980). As in their results, the array of white dots corresponds to the projection down the *c*-axis of the empty *A*-sites in the structure, these corresponding to the regions of lowest electric potential in the structure. The sense of the contrast is confirmed by the fact that the cores of the dislocations observed also appear white. We reproduce here only two small fields that contain dislocations: these are of two kinds that were observed with about equal frequency and are typified by figs. 4*a* and *b*.

In fig. 4*a* the most obvious departures from regularity in the array are two extra half-rows of white dots (indicated by black arrows) which include an angle of 56°, which are most clearly seen by viewing the photograph at an oblique angle along the direction of the arrows. In the disturbed region near the junction of these half-rows the white dots are enlarged. The half-rows clearly correspond to half-planes of *A*-sites lying on (110) and (1$\bar{1}$0).

Interpretation by means of the cardboard cut-outs is shown in figs. 5 and 6. Careful comparison of fig. 5 with fig. 4*a* shows that the essential nature of the dislocation involves the insertion of an extra half-plane of complete unit cells along a (100) plane bisecting the acute angle between the 'obvious' half-planes of *A*-sites on (110) and (1$\bar{1}$0). This involves two extra half-rows of white dots indicated by the broad arrow, which can again be seen by viewing obliquely in the direction of this arrow. The pattern of enlarged holes in the core of the dislocation depends on the distribution of the strain field around it. In fig. 5*a* this has been arranged so that these holes form an extension of one of the extra half-planes of *A*-sites beyond its intersection

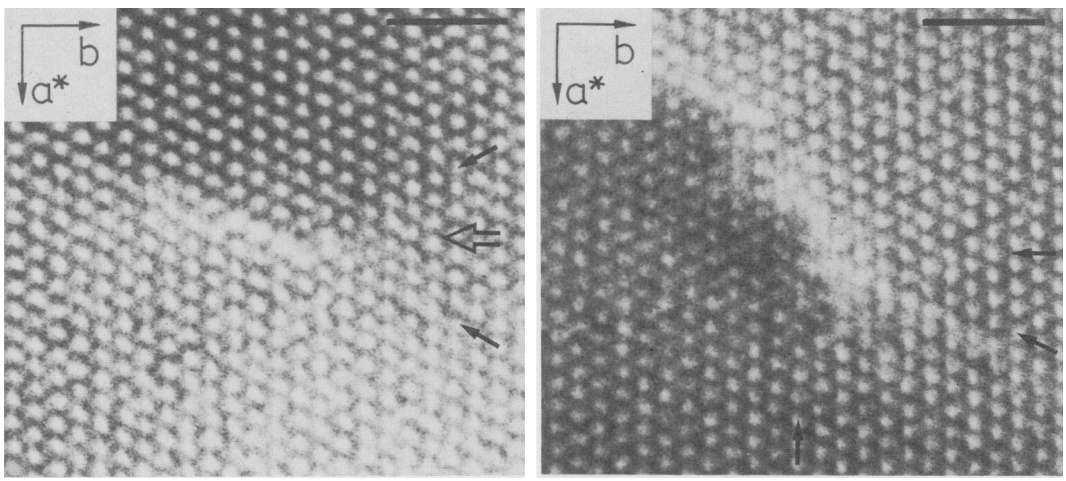

FIG. 4. Section of grunerite viewed down [001] showing dislocations, (*left*) with Burgers vector **a**, and (*right*) with Burgers vector $\frac{1}{2}\mathbf{a}+\frac{1}{2}\mathbf{b}$. Single arrows mark extra half-rows of *A*-sites. Scale bars 50 Å.

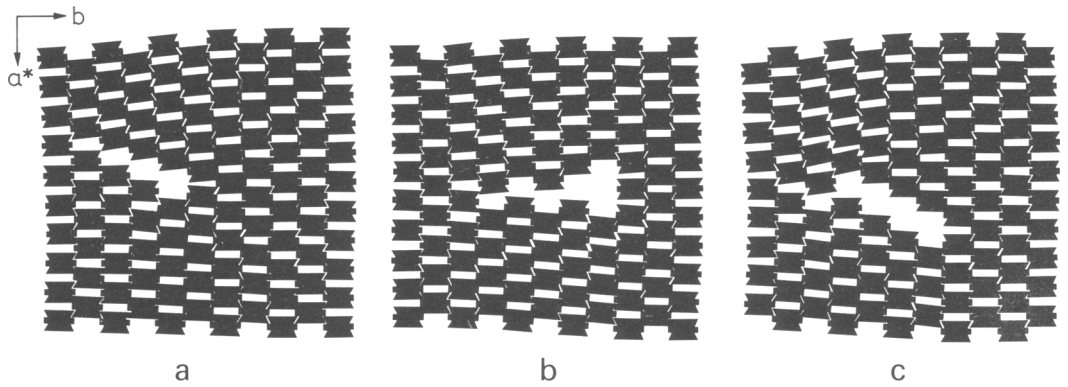

FIG. 5. Models of a dislocation with Burgers vector **a**. The arrangement of the enlarged holes is very sensitive to the disposition of the strain, as shown by the variations between (*a*), (*b*), and (*c*). These figures are best viewed at an oblique angle from the right-hand side.

with the other, as in fig. 4*a*. In fig. 5*b* the strain has been made symmetrical about the half-plane of extra cells on (100), and this leads to enlarged holes on a continuation of the trace of this plane. In fig. 5*c* the strain is so arranged that the enlarged holes lie on one extra half-plane of *A*-sites before its intersection with the other. The arrangements that have been observed in electron micrographs extend over this range of strain distributions.

The nature of this dislocation merits some discussion. It clearly lies on [001], and its Burgers vector clearly has a component $a \sin \beta$ in the **a*** direction perpendicular to [001]. No more than this can be observed directly from the photograph. However, it is clear from fig. 7 that if a half-plane of unit cells terminating along a [001] line is inserted on a (100) plane in a monoclinic structure then the Burgers vector will be **a**. The point A′ has to be displaced from the previously coincident point A in the process of inserting the half-plane, and although this displacement has a component parallel to the dislocation it does not lead to a step on the (001) face, because of the β angle of the inserted cells. The configuration therefore has the characteristics of an edge dislocation appropriate to a non-orthogonal crystal system. It seems convenient to describe it as a non-orthogonal edge dislocation on [001] with Burgers vector **a**. Similar problems arose in the description of the dislocation-like character of some of the 'incoherent' terminations of lamellae of multiple *I*-beams described previously (Whittaker *et al.*, 1981).

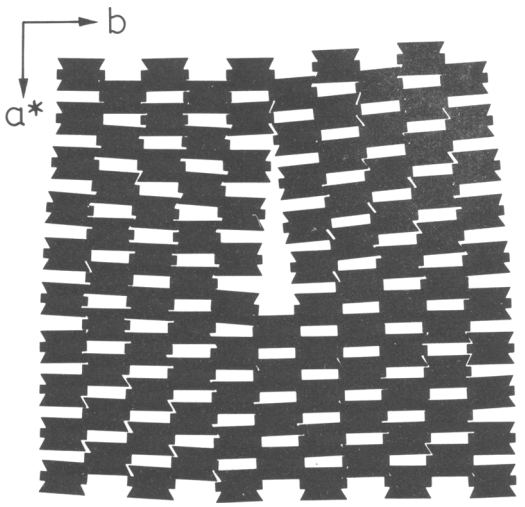

FIG. 6. Model of a dislocation with Burgers vector $\frac{1}{2}\mathbf{a}+\frac{1}{2}\mathbf{b}$.

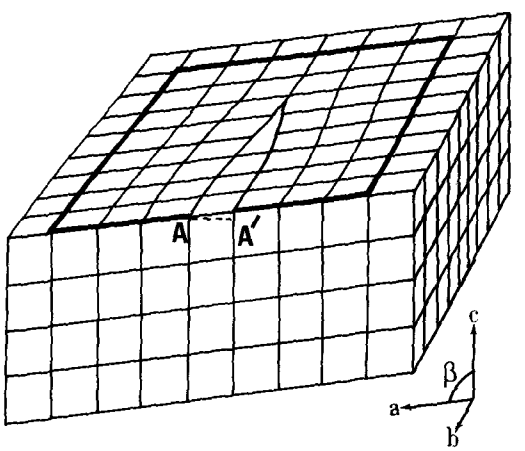

FIG. 7. A 'non-orthogonal edge dislocation' in a monoclinic lattice.

If a dislocation is constructed with an extra half-plane of *I*-beams (half-unit cells) on (010), as in fig. 6, then the strain must be unsymmetrical across this plane in order to permit the *I*-beams on opposite sides of the gap to take up a glide relationship to one another instead of a mirror relationship. This involves the introduction of another extra half-plane of *I*-beams on (100), so that it is a non-orthogonal edge dislocation on [001] with a Burgers vector $\frac{1}{2}\mathbf{a}+\frac{1}{2}\mathbf{b}$, which is of course a lattice vector in the *C*-centred lattice. Such a dislocation is present on fig. 4*b*, the most obvious evidence of its presence being extra half-rows of white dots corresponding to extra half-planes of *A*-sites along (110) and (010) which are arrowed. The extra half-plane of *I*-beams along (100) also leads to an extra half-row of white dots (also arrowed) in this orientation, but this is difficult to see. All of these effects are best viewed obliquely along the direction of the arrows.

The introduction of an extra half-plane of complete unit cells on (010) would lead to two extra half-planes of *A*-sites on (110) and (1$\bar{1}$0) including an obtuse angle (124°). However, this would involve a much larger Burgers vector **b** (of length 18 Å), and has not been observed. The lengths of the Burgers vectors of the dislocations in fig. 4 are both of the order of 9–10 Å.

Acknowledgements. This work forms part of an investigation financed by a research grant from NERC which is gratefully acknowledged. One of us (J.L.H) acknowledges financial support from the SRC.

REFERENCES

Alario Franco, M., Hutchison, J. L., Jefferson, D. A., and Thomas, J. M. (1977). *Nature*, **266**, 520–1.

Buseck, P. R. and Iijima, S. (1974). *Am. Mineral.* **59**, 1–21 [MA74–1910].

Chisholm, J. E. (1973). *J. Materials Sci.* **8**, 475–83 [MA74–1916].

Hutchison, J. L., Irusteta, M. C., and Whittaker, E. J. W. (1975). *Acta. Crystallogr.* **31A**, 794–801 [MA76–2344].

Jefferson, D. A., Mallinson, L. G., Hutchison, J. L., and Thomas, J. M. (1978). *Contrib. Mineral. Petrol.* **66**, 1–4.

Mallinson, L. G., Jefferson, D. A., Thomas, J. M., and Hutchison, J. L. (1980). *Phil. Trans. R. Soc.* **295**, 537–52.

Papike, J. J. and Ross, M. (1970). *Am. Mineral.* **55**, 1945–72 [MA 71–1751].

Taylor, H. F. L. (1959). Personal communication, also reported in Hodgson, A. A., 1965 Roy. Inst. Chem. Lec. Series 4: 'Fibrous Silicates' p. 12.

Thompson, J. B., *Jr.* (1978). *Am. Mineral.* **63**, 239–49 [MA 78–4032].

Veblen, D. R. and Buseck, P. R. (1979). Ibid. **64**, 687–700 [MA 80–1239].

—— —— (1980). Ibid. **65**, 599–623.

—— —— and Burnham, C. W. (1977). *Science*, **198**, 359–65 [MA 78–3473].

Warren, B. E. (1929). *Z. Krist.*, **27**, 42–57 [MA 4, 201].

Whittaker, E. J. W., Cressey, B. A., and Hutchison, J. L. (1981). *Min. Mag.* **44**, 27–35.

[*Manuscript received 10 October 1980; revised 9 February 1981*]